Journal of Photochemistry & Photobiology, B: Biology 238 (2023) 112617

Contents lists available at ScienceDirect

Journal of Photochemistry & Photobiology, B: Biology

journal homepage: www.elsevier.com/locate/jphotobiol

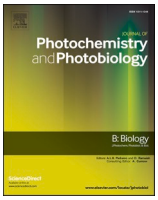

Blue light pollution causes retinal damage and degeneration by inducing ferroptosis

Xuan Li [a], Sen Zhu [b,c,*], Fujian Qi [b]

[a] Lanzhou University Second Hospital, Lanzhou, China
[b] School of Life Sciences, Lanzhou University, Lanzhou, China
[c] Zhongshan School of Medicine, Sun Yat-Sen University, Guangzhou, China.

ARTICLE INFO

Keywords:
Light pollution
Blue light
Retina
Ferroptosis
Lipid peroxidation

ABSTRACT

With the development of technology and electronic products, the problem of light pollution is becoming more and more serious. Blue light, the most energetic light in visible light, is the main culprit of teenage vision problems in the modern environment. As the tissue with the highest oxygen consumption, the retina is vulnerable to oxidative stress. However, the exact way in which blue light-triggered reactive oxygen species (ROS) cause retinal cell death remains unclear. Ferroptosis is a newly defined cell death pathway, whose core molecular mechanism is cell death caused by excessive lipid peroxidation. In this study, the results indicated that blue light-triggered ROS burst in retinal cells, in the meantime, intracellular Fe^{2+} levels were also significantly up-regulated. Further, deferoxamine (DFO) significantly improved blue light-triggered lipid peroxidation and cell death in ARPE-19 cells, and ferrostatin-1 (Fer-1) alleviated retinal oxidative stress and degeneration in rats. Furthermore, the GSH-GPX4 and FSP1-CoQ_{10}-NADH systems served as key systems for cellular defense against ferroptosis, and interestingly, our results demonstrated that blue light triggered imbalance of the GSH-GPX4 and FSP1-CoQ_{10}-NADH systems in retinal cells. Taken together, these pieces of evidence suggest that ferroptosis may be a crucial pathway for blue light-induced retinal damage and degeneration, which helps us to understand exactly why blue light pollution causes visual impairment in adolescents.

1. Introduction

Air pollution, noise pollution, and water pollution are considered to be the most important sources of pollution in past years (1). However, with the development of electronic products, the adverse consequences caused by light pollution are becoming increasingly serious. As the most energetic electromagnetic wave in visible light, blue light popularly exists in a variety of modern electronic products, including smartphones, laptops, and tablets (2). Compared with ultraviolet rays (UV), blue light has stronger penetration and is more common in daily life (3). Short-wavelength blue light has been reported to have apparent retinal phototoxicity (4). The retina, as the most oxygen-consuming tissue in vivo, is vulnerable to oxidative stress (5,6). Blue light-induced mitochondrial damage and ROS burst are recognized as important causes of retinal degeneration (7). In addition, ROS-mediated activation of apoptotic signaling was recognized in the past as a primary molecular mechanism of blue light-triggered retinal degeneration (8,9). Notably, blue light-triggered ROS burst and excessive lipid peroxidation, as well as disruption of redox status (10,11), imply that other types of cell death processes may also be involved in blue light-triggered retinal degeneration, not only classical apoptosis.

Ferroptosis, a nonapoptotic cell death, was proposed in 2012 by Dixon et al. (12) and is marked as the disruption of redox balance, resulting in excessive lipid peroxidation and ultimately cell death. High levels of intracellular Fe^{2+} can generate abundant ROS through the Fenton reaction, leading to lipid peroxidation, which is pivotal to ferroptosis (13). However, there are some natural antioxidant systems in cells, such as the GSH-GPX4 (glutathione peroxidase 4) and FSP1 (ferroptosis suppressor protein 1)-CoQ_{10}-NADH antioxidant systems. The GSH-GPX4 antioxidant system reduces lipid peroxides (LPOs) accumulation and protects against ferroptosis by transforming intracellular LPOs into the corresponding alcohols (14). On the other hand, Marshall et al. (15) earlier revealed that FSP1 functions as an NADH-dependent CoQ oxidoreductase in vitro. Reduced CoQ acts as an antioxidant, and Shimada et al. (16) demonstrated that its soluble analogue, idebenone, effectively inhibits lipid peroxidation and ferroptosis. Recently, Doll

* Corresponding author at: School of Life Sciences, Lanzhou University, Lanzhou, China.
E-mail address: zhus19@lzu.edu.cn (S. Zhu).

https://doi.org/10.1016/j.jphotobiol.2022.112617
Received 11 September 2022; Received in revised form 20 November 2022; Accepted 1 December 2022
Available online 5 December 2022

et al. (17) and Bersuker et al. (18) comprehensively revealed the function of the FSP1-CoQ_{10}-NADH system as another important molecular mechanism inhibiting ferroptosis, independent of the GSH-GPX4 antioxidant system.

In this research, we studied the effect of blue light on intracellular Fe^{2+} levels, lipid peroxidation, as well as GSH-GPX4 and FSP1-CoQ_{10}-NADH systems, and revealed the role of ferroptosis in blue light-triggered retinal degeneration. This study can help us better understand the reasons for retinal degeneration caused by blue light and provide us with new insights into preventing blue light pollution.

2. Materials and methods

2.1. Materials

FeRhoNox™-1 (Serve Life science, Shanghai, China). DCFH-DA (St. Louis, MO, USA). Anti-GPX4 antibody, GSH/GSSG assay kit, and NAD^+/NADH assay kit (Beyotime, Shanghai, China). Propidium iodide (PI) and 2-(4-Amidinophenyl)-6-indolecarbamidine (DAPI) (Beyotime, Shanghai, China). Anti-AIFM2/AMID and Anti-β-Tubulin antibodies (Santa Cruz Biotechnology, CV, USA). Anti-4-Hydroxynonenal (4-HNE) antibody (Invitrogen, Massachusetts, USA). CoQ_{10} ELISA kit (COBIO, Shanghai, China). Iron assay kit (Abcam, Cambridge, UK). C11 BODIPY 581/591 (Mao Kang Biotechnology, Shanghai, China). Trypsin-EDTA Solution (Beijing T&L Biological Technology Co., Ltd., Beijing, China). Fetal bovine serum (CellMax, Beijing, China). Bovine serum albumin (BAS) (Sigma-Aldrich, MO, USA). LED blue light (435–445 nm) (JDL company, Hangzhou, China). Cell culture flask and cell culture plates (Nest Biotechnology, Wuxi, China).

2.2. Cell culture and treatment

ARPE-19 cells were cultured at 37 °C in an incubator containing 5% CO_2. Cells were incubated with DFO for 3 h and irradiated with blue light (435–445 nm, 11.2 W/m^2) for the subsequent 12 h. In the MTT analysis experiments, ARPE-19 cells (5000 cells/well) were seeded in 96-well plates for 24 h, incubated for 3 h with or without DFO, and then exposed to the blue light for 12 h. For other experiments, such as DAPI/PI staining, lipid peroxidation analysis, GSH/GSSG analysis, and intracellular Fe^{2+} levels analysis, etc., cells were seeded in 6-well plates. When the cell reached 60%–70% confluence, the cells were treated with DFO for 3 h and blue light for 12 h, and the cells were collected for subsequent experiments subsequently. The cell lines were authenticated at VivaCell Shanghai using short tanderrepeat analysis (STA).

2.3. Detection of Fe^{2+} levels

ARPE-19 cells were seeded in 6-well plates and pretreated with DFO for 3 h, and then exposed to blue light for 12 h. After washing cells three times with PBS, the cells were incubated with FeRhoNox™-1 (5 μM) for 30 min. After that, DAPI was used to counterstain the cell nucleus, which were immediately observed and imaged under a fluorescence microscope (IX71, Olympus).

2.4. Determination of ROS

ARPE-19 cells were treated with DFO for 3 h and then exposed to blue light for 12 h. Then, DCFH-DA probe was incubated with the cells for 15 min, and DCF fluorescence was detected by the fluorescence microscope (IX71, Olympus).

2.5. Detection of lipid peroxidation

Intracellular lipid peroxidation levels were analyzed by intracellular malondialdehyde (MDA) levels and C11-BODIPY 581/591 fluorescence intensity. The MDA contents were detected according to the manufacturer's instructions. Measure absorbance at 532 nm. Moreover, ARPE-19 cells were incubated with C11 BODIPY and DAPI for 20 min, and then confocal imaging was performed (A1R + Ti2-E, Nikon).

2.6. Cell viability analysis

MTT assay and lactic dehydrogenase (LDH) release were used to assess cell viability. After cell was treated, 1 mg/ml MTT solution (dissolved in the medium) was added and continued the incubation for 4 h. MTT solution was poured out, 150 μL DMSO was added, and then absorbance was measured at 470 nm wavelength after 10 min oscillation. LDH release is widely used in the assessment of cytotoxicity. LDH release was detected by the kit and the absorbance was measured at 490 nm.

2.7. Cell death analysis

ARPE-19 cells were seeded in 6-well plates for 24 h. The cells were pretreated with DFO for 3 h and then exposed to blue light for 12 h. After washing cells three times with PBS, the cells were incubated with PI (10 μg/ml) for 15 min. After that, with DAPI (5 μg/ml) counterstained-cell nucleus, the cells were immediately observed under the fluorescent microscope. Three photos were obtained per well for statistical analysis. Each experiment was repeated at least three times.

2.8. Immunofluorescence

The operations were as described in our previous study (19). In brief, cells were fixed with 4% PFA and then blocked with 1% BSA. Then, cells were incubated with the corresponding primary and fluorescent secondary antibodies. Subsequently, the nuclei were stained with DAPI, and a fluorescent signal was observed by fluorescence microscope (A1R + Ti2-E, Nikon).

2.9. Detection of GSH and GSSG levels

Cells were collected after treatment and then detected by a GSH/GSSG assay kit. Intracellular GSH content can be calculated according to the content of total glutathione and GSSG.

2.10. Detection of NADH and NAD^+ levels

The WST-8 assay was used to examine the NADH and NAD^+ levels through kit. Measure absorbance at 450 nm.

2.11. Animals and treatment

Fifteen Sprague–Dawley rats were obtained from the Animal Experiment Center of Lanzhou University and randomly assigned to 3 groups (5 rats/group). CTR, control group; BL, blue light irradiation group; BL + Fer-1, pre-injection of Fer-1 (dissolved in normal saline) and blue light irradiation group. Rats were injected intraperitoneally with or without Fer-1 (2 mg/kg/day) for 7 days, after which they rats were irradiated with blue light for 8 h. Rats were immobilized during blue light irradiation, as described in the previous study (4). Rats were euthanized by intraperitoneal injection of sodium pentobarbital (200 mg/kg).

2.12. Retinal morphology analysis

Eye tissue was sectioned, stained with H&E staining, and then imaged by a microscope (BX53, Olympus). Slicing operations and photo acquisition locations were as described in our previous studies (4). The retinal thickness was photographed every 50 μm near the optic disc, and three pictures were taken in each direction. Retinal thickness was analyzed by Image J software.

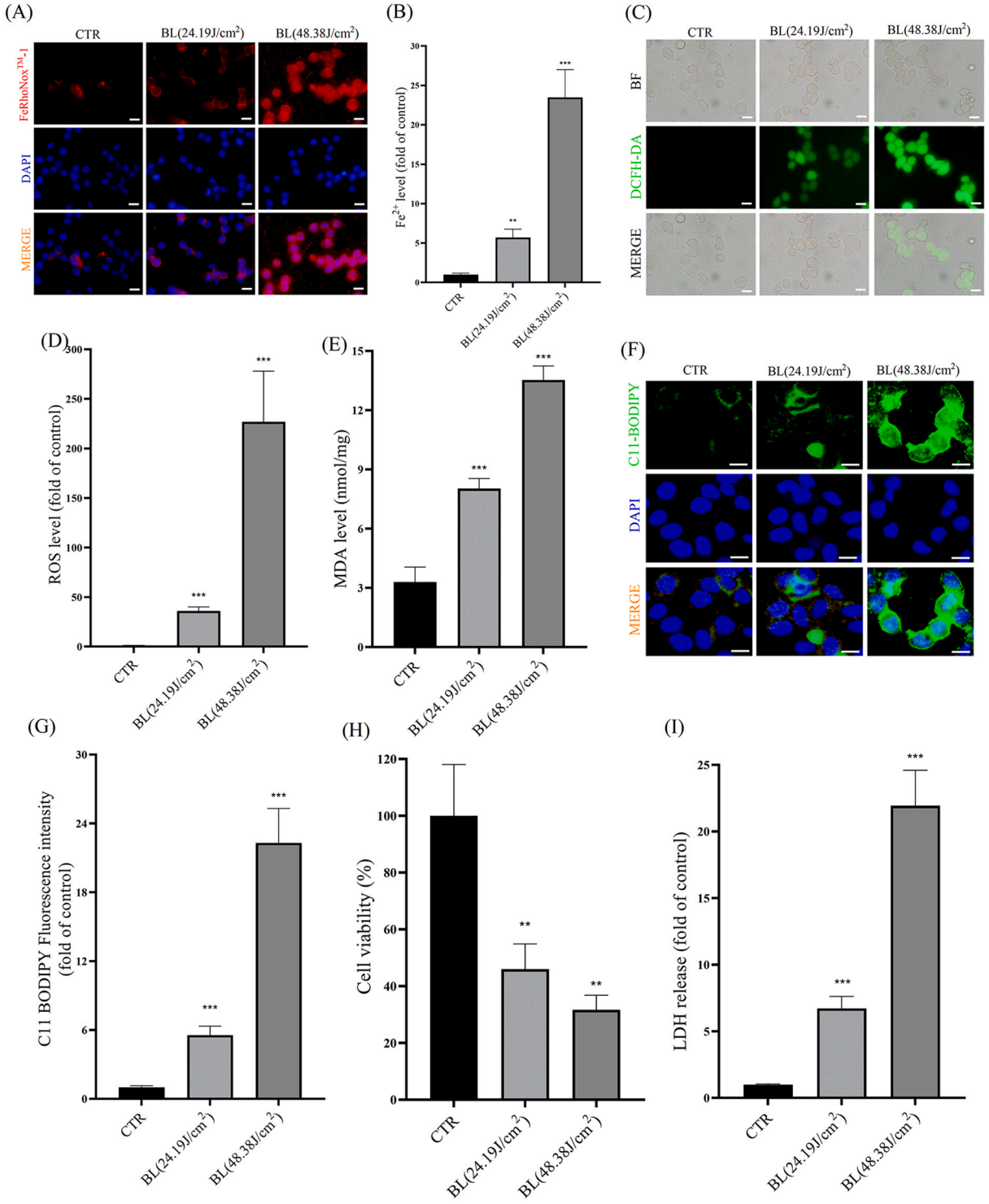

Fig. 1. Blue light induces Fe^{2+} burst, lipid peroxidation, and decreased cell viability. (A) FeRhoNox™-1 probe was incubated with ARPE-19 cells, and then intracellular Fe^{2+} level was observed by fluorescence microscope. Scale bar = 20 μm. (B) Statistics of Fe^{2+} fluorescence intensity. (C) DCFH-DA probe was incubated with ARPE-19 cells and intracellular ROS was observed by the fluorescence microscope. Scale bar = 20 μm. (D) Statistics of DCFH-DA fluorescence intensity. (E) Intracellular MDA content alteration. (F) Cells were incubated with C11 BODIPY and DAPI and subsequently detected by fluorescence microscopy. Scale bar = 10 μm. (G) Statistics of C11 BODIPY fluorescence intensity. (H) Cell viability was detected by MTT. (I) LDH release was performed to analyze the cytotoxicity. $^{**}p < 0.01$, $^{***}p < 0.001$ vs. CTR. (For interpretation of the references to colour in this figure legend, the reader is referred to the web version of this article.)

2.13. Intraretinal ROS analysis

Retinal tissue was cryosectioned and then the frozen slides were returned to room temperature. Liquid was eliminated, and the target tissue was marked with a liquid blocker pen. Incubate with an autofluorescence quencher for 5 min. DHE staining solution was incubated with the marker at 37 °C for 30 min. Subsequently, DHE fluorescence was observed by fluorescence microscopy (IX71, Olympus).

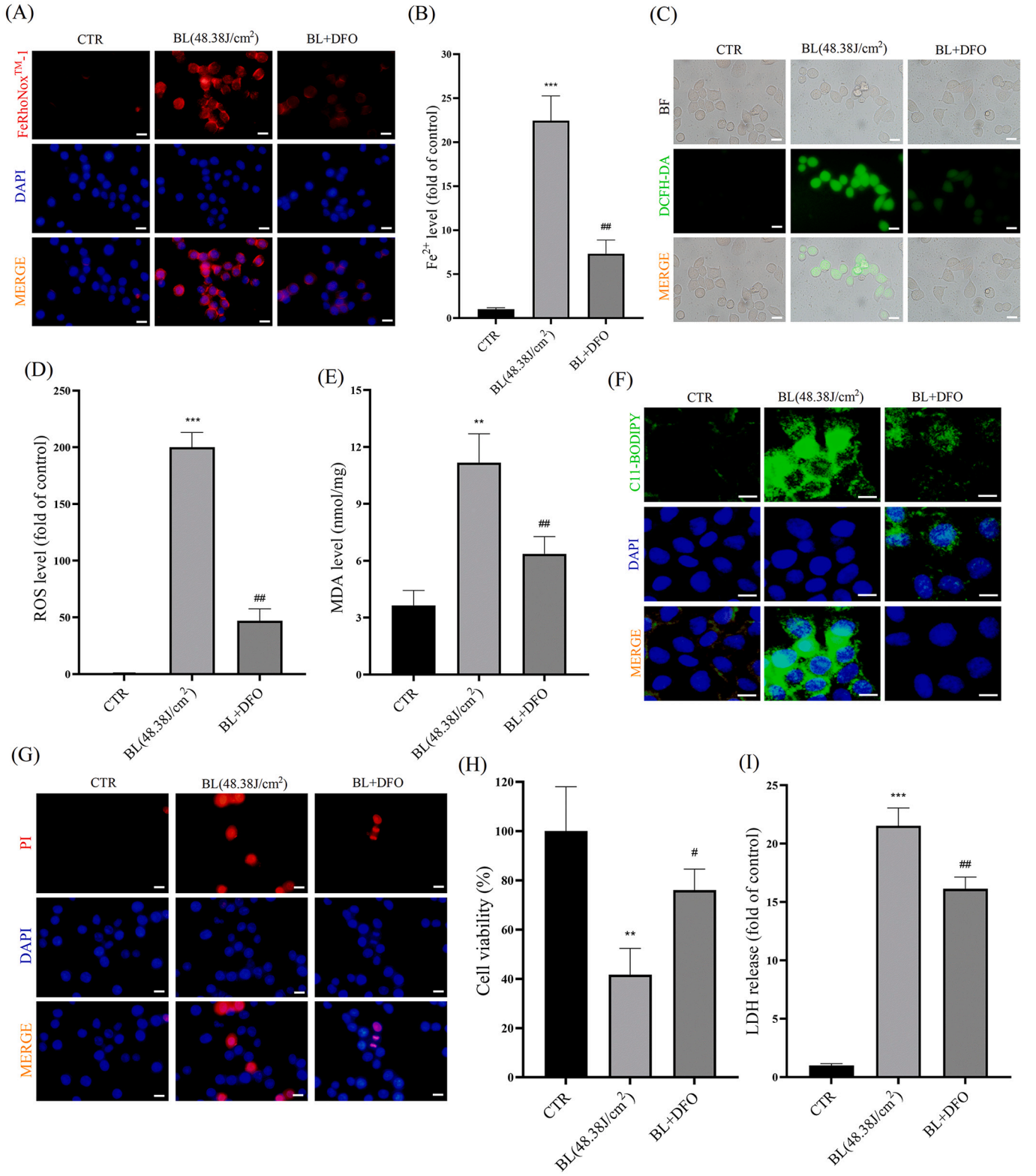

Fig. 2. Deferoxamine alleviates blue light-induced lipid peroxidation and cell death. (A) Intracellular Fe^{2+} was labeled with FeRhoNox™-1 probe and detected by fluorescence microscopy. Scale bar = 20 μm. (B) Statistics of Fe^{2+} fluorescence intensity. (C) Intracellular ROS was labeled with DCFH-DA probe and observed under the fluorescence microscopy. Scale bar = 20 μm. (D) Statistics of DCFH-DA fluorescence intensity. (E) Intracellular MDA content alteration. (F) Cells were incubated with C11 BODIPY and DAPI and detected by fluorescence microscopy. Scale bar = 10 μm. (G) Cell death was analyzed by PI/DAPI staining. Scale bar = 20 μm. (H) Cell viability was detected by MTT. (I) LDH release was performed to analyze the cytotoxicity. $^{**}p < 0.01$, $^{***}p < 0.001$ vs. CTR; $^{\#}p < 0.05$, $^{\#\#}p < 0.01$ vs. BL. (For interpretation of the references to colour in this figure legend, the reader is referred to the web version of this article.)

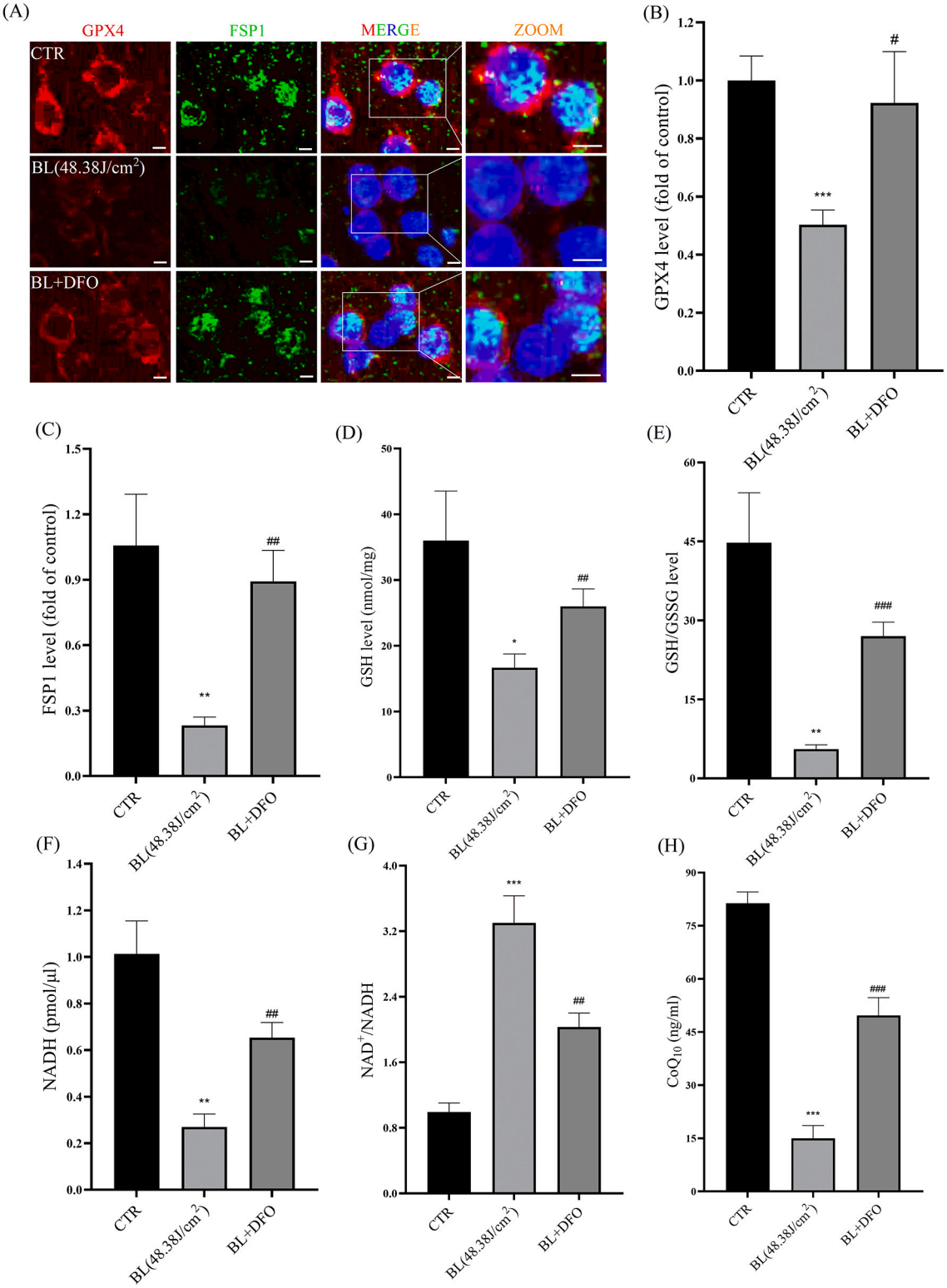

Fig. 3. Blue light disrupts the GSH-GPX4 and FSP1-CoQ_{10}-NADH system. (A) Intracellular GPX4 and FSP1 expressions were examined by immunofluorescence. Scale bar = 5 μm. (B) Statistics of GPX4 level. (C) Statistics of FSP1 level. (D) Intracellular GSH content alteration. (E) Statistics of GSH/GSSG ratio. (F) Intracellular NADH content alteration. (G) Statistics of NAD^+/NADH ratio. (H) Intracellular CoQ10 activity alteration. $^*p < 0.05$, $^{**}p < 0.01$, $^{***}p < 0.001$ vs. CTR; $^{\#}p < 0.05$, $^{\#\#}p < 0.01$, $^{\#\#\#}p < 0.001$ vs. BL. (For interpretation of the references to colour in this figure legend, the reader is referred to the web version of this article.)

2.14. Data statistics and analysis

All experiments were repeated at least three times independently ($n \geq 3$). Data showed as mean ± standard deviation (SD) and were analyzed by Student's *t*-test, with differences of $p < 0.05$ considered statistically significant.

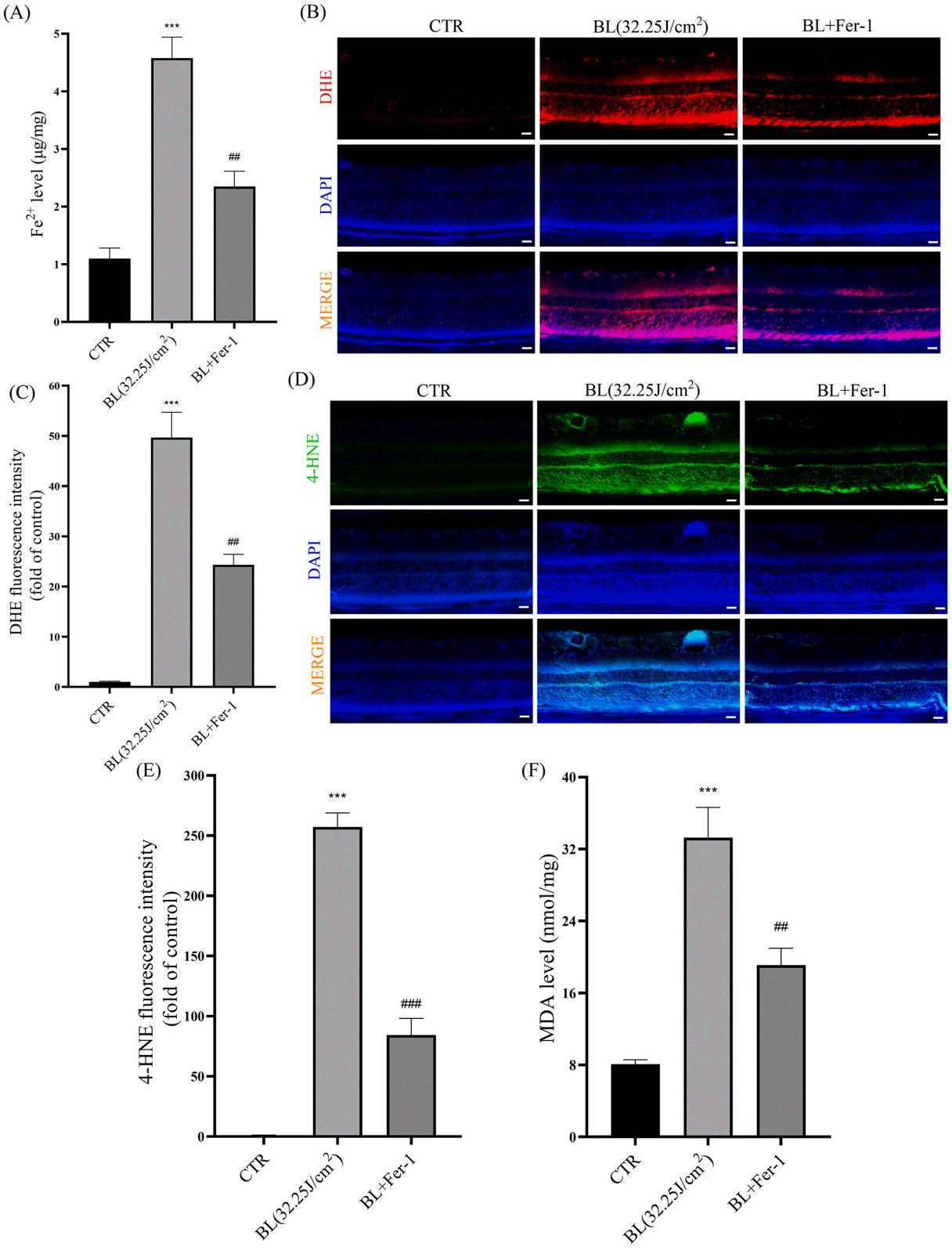

Fig. 4. Ferrostatin-1 ameliorates blue light-triggered retinal oxidative damage. (A) Fe^{2+} level alteration was assessed in rat retinal. (B) DHE probes were used to label ROS in the retina and then detected by fluorescence microscopy. Scale bar = 20 μm. (C) Statistics of DHE fluorescence intensity. (D) The intraretinal 4-HNE level was detected by immunofluorescence. Scale bar = 20 μm. (E) Statistics of 4-HNE fluorescence intensity. (F) Intraretinal MDA content alteration. $^{***}p < 0.001$ vs. CTR; $^{\#\#}p < 0.01$ vs. BL. (For interpretation of the references to colour in this figure legend, the reader is referred to the web version of this article.)

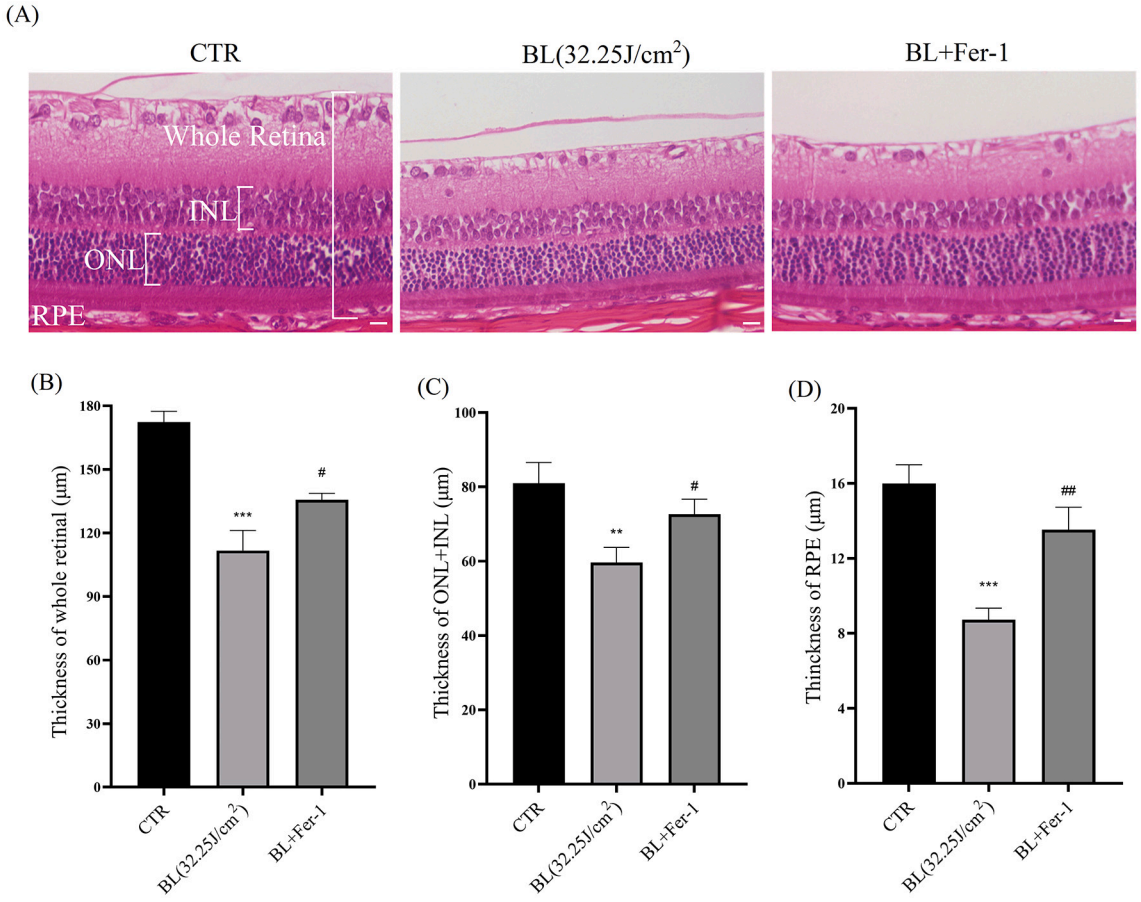

Fig. 5. Ferrostatin-1 improves blue light-triggered retinal degeneration. (A) H&E staining was performed to analyze retinal morphology. Scale bar = 20 μm. (B) Alteration of whole retinal thickness. (C) Alteration of ONL and INL thickness. (D) Alteration of RPE layer thickness. $^{**}p < 0.01$, $^{***}p < 0.001$ vs. CTR; $^{\#}p < 0.05$, $^{\#\#}p < 0.01$ vs. BL. (For interpretation of the references to colour in this figure legend, the reader is referred to the web version of this article.)

3. Results

3.1. Blue light induces Fe^{2+} burst, lipid peroxidation, and decreased cell viability

ARPE-19 cells were treated with blue light for 6 h or 12 h and then incubated with the Fe^{2+} probe FeRhoNox™-1 in the dark and subsequently detected by fluorescence microscopy. Blue light significantly triggered intracellular Fe^{2+} burst (Fig. 1(A)-1(B)). Intracellular ROS levels were analyzed by DCFH-DA fluorescence, and the results indicated that blue light remarkably triggered ROS burst (Fig. 1(C)-1(D)). Moreover, intracellular lipid peroxidation was analyzed by MDA contents and the C11 BODIPY fluorescence signal, which showed that blue light caused LPOs accumulation (Fig. 1(E)-1(G)). Cell viability was analyzed by MTT assay and LDH release, and results showed that cell viability was significantly reduced after exposure to blue light (Fig. 1(H)-1(I)). High levels of Fe^{2+} lead to excessive lipid peroxidation and cell death, which is a hallmark event of ferroptosis. Therefore, we speculate that ferroptosis may be a critical molecular mechanism in blue light-triggered retinal degeneration.

3.2. Deferoxamine relieves blue light-triggered lipid peroxidation and cell death

To confirm that ferroptosis was involved in blue light-triggered retinal degeneration, deferoxamine (DFO) was used to treat cells. As expected, the blue light-induced elevation of intracellular Fe^{2+} level was significantly inhibited by DFO (Fig. 2(A)-2(B)). Moreover, DFO significantly alleviated blue light-triggered intracellular ROS burst and LPOs accumulation (Fig. 2(C)-2(F)). Furthermore, cell viability and death were analyzed by DAPI/PI staining, MTT assay, and LDH release. The results showed that DFO remarkably alleviated cell death and improved cell viability in ARPE-19 cells (Fig. 2(G)-2(I)). The above evidence confirms that blue light elevates intracellular Fe^{2+} levels, which further leads to intracellular ROS burst and excessive lipid peroxidation, ultimately inducing ferroptosis.

3.3. Blue light disrupts the GSH-GPX4 and FSP1-CoQ_{10}-NADH systems in ARPE-19 cells

There are some natural redox regulatory systems in cells, such as the GSH-GPX4 and FSP1-CoQ_{10}-NADH systems, which can reduce the accumulation of LPOs and thus resist ferroptosis (20). We further investigated the effect of blue light on the GSH-GPX4 and FSP1-CoQ_{10}-NADH systems. Immunofluorescence analysis showed that the expression of GPX4 and FSP1 was significantly inhibited by blue light (Fig. 3(A)-3(C)). Moreover, we assessed the intracellular GSH and NADH levels, and CoQ_{10} activity. The results showed that blue light decreased GSH and NADH levels, down-regulated GSH/GSSG ratio, up-regulated NAD^+/NADH ratio, and reduced CoQ_{10} activity (Fig. 3(D)-3(H)). Notably, these processes can be reversed by the DFO, and it is clear that high level of Fe^{2+} is the direct factor leading to the imbalance of the GSH-GPX4 and FSP1-CoQ_{10}-NADH systems.

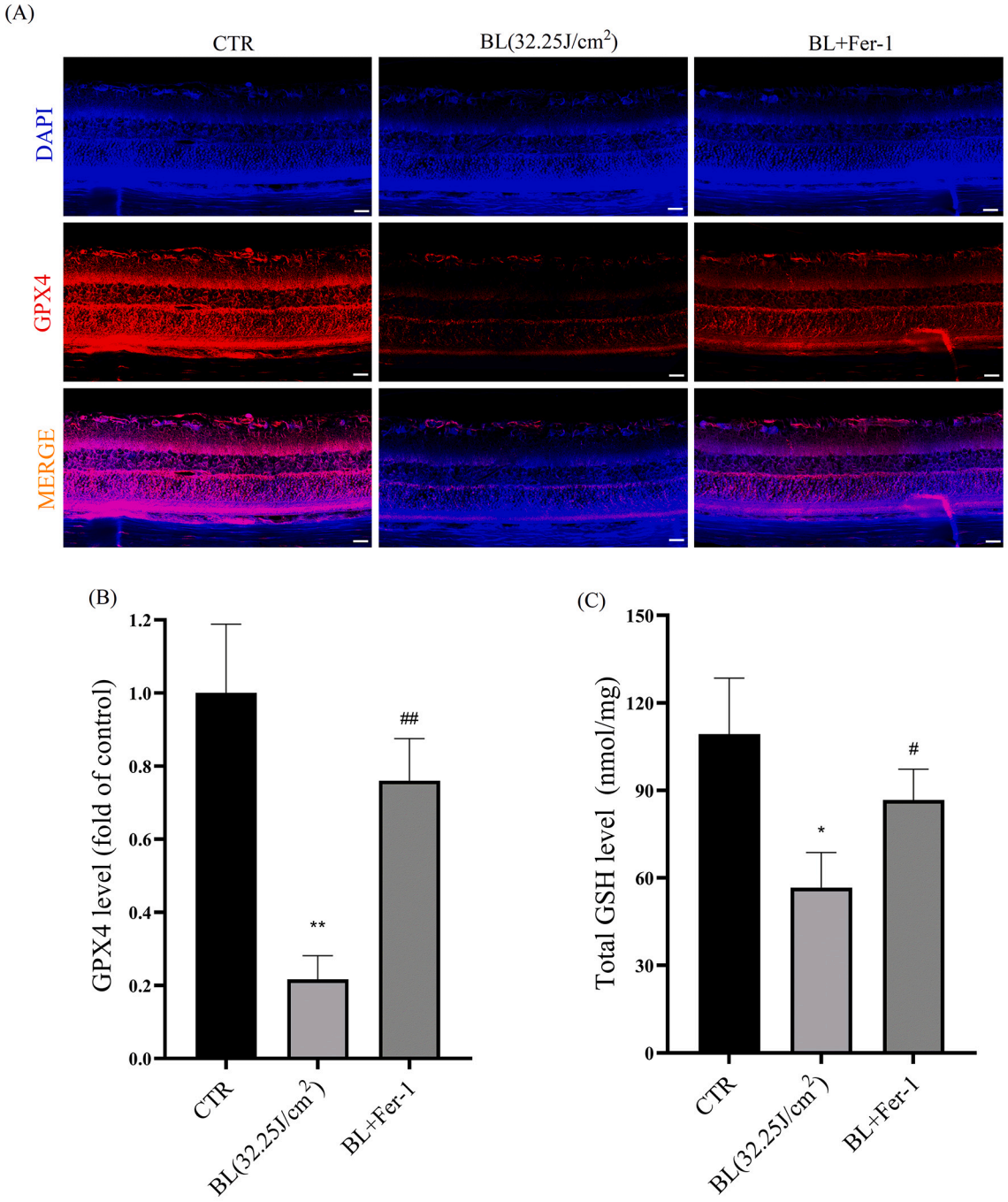

Fig. 6. Blue light disrupts the GSH-GPX4 system in rat retina. (A) GPX4 expression was detected by immunofluorescence in the rat retina. Scale bar = 20 μm. (B) Statistics of GPX4 fluorescence intensity. (C) Total GSH levels alteration. $^{*}p < 0.05$, $^{**}p < 0.01$ vs. CTR; $^{\#}p < 0.05$, $^{\#\#}p < 0.01$ vs. BL. (For interpretation of the references to colour in this figure legend, the reader is referred to the web version of this article.)

3.4. Blue light induces retinal damage and degeneration by inducing ferroptosis in rats

Next, in vivo experiments were performed to study the role of ferroptosis in blue light-triggered retinal degeneration. We found that blue light significantly triggered Fe^{2+} level increase in the retina, which could be relieved by ferrostatin-1 (Fer-1) (Fig. 4(A)). Moreover, DHE probes were used to label ROS in cryosectioned retinal tissue, and the data showed that Fer-1 significantly inhibited intraretinal ROS burst (Fig. 4(B)-4(C)). 4-Hydroxynonena (4-HNE) levels and MDA contents were used to analyze the level of lipid peroxidation in rat retina. It was found that Fer-1 significantly alleviated lipid peroxidation and reduced the accumulation of LPOs (Fig. 4(D)-4(F)). Furthermore, the results showed that Fer-1 restored retinal thickness and improved retinal degeneration, including the whole retina, outer nuclear layer (ONL), inner nuclear layer (INL), and pigment epithelial cell layer (RPE), and so on (Fig. 5(A)-5(D)).

In vitro, we revealed that blue light disrupts the GSH-GPX4 and FSP1-CoQ_{10}-NADH systems, therefore, we proceeded to explore whether blue light influences these two systems in vivo. We found that blue light remarkably inhibited GPX4 expression and down-regulated GSH levels (Fig. 6(A)-6(C)). On the other hand, blue light significantly suppressed FSP1 expression, reduced NADH levels, increased the NAD^{+}/NADH ratio, and decreased CoQ_{10} activity (Fig. 7(A)-7(E)). Notably, these

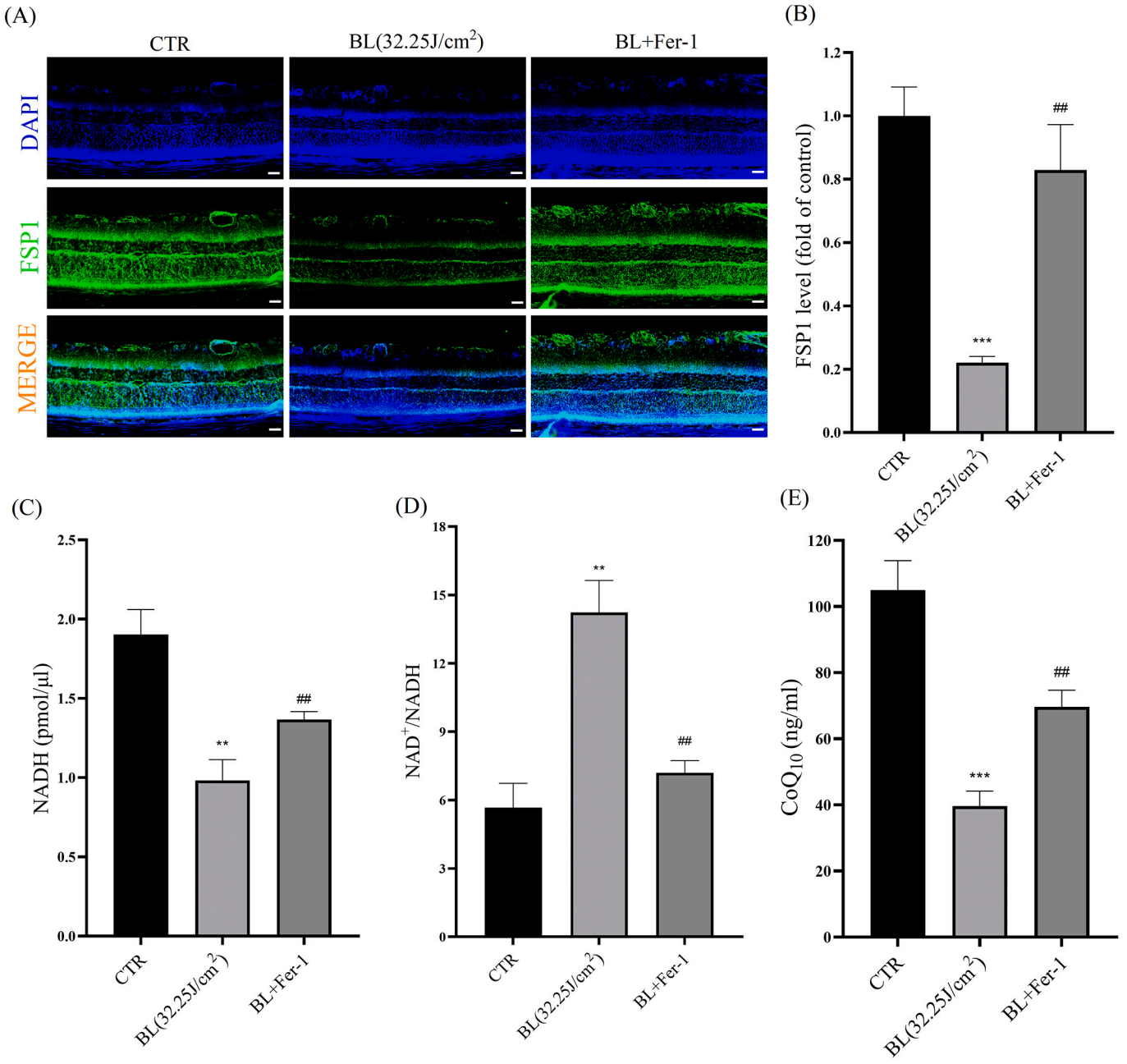

Fig. 7. Blue light disrupts the FSP1-CoQ_{10}-NADH system in rat retina. (A) FSP1 expression was detected by immunofluorescence. Scale bar = 20 μm. (B) Statistics of FSP1 fluorescence intensity. (C) Intraretinal NADH content alteration. (D) Statistics of NAD^+/NADH ratio. (E) Intraretinal CoQ10 activity alteration. $^{**}p < 0.01$, $^{***}p < 0.001$ vs. CTR; $^{\#\#}p < 0.01$ vs. BL. (For interpretation of the references to colour in this figure legend, the reader is referred to the web version of this article.)

metabolic processes could be reversed by Fer-1, supporting the speculation in this study that blue light induced ferroptosis in retinal cells. In summary, these results uncover that ferroptosis is a key pathway by which blue light induces retinal degeneration.

4. Discussion and conclusion

Oxidative stress and oxidative damage caused by blue light-induced intracellular ROS burst are key causes of retinal degeneration (21–28). Previous studies have illustrated that activation of apoptotic signals, including ER stress (28), autophagy (9,24), and caspase-3 mediated apoptosis (29), et., is a potential mechanism of retinal degeneration triggered by blue light, and the activation of these apoptotic signals is closely related to the high level of intracellular ROS. However, cell death led by high-level ROS does not appear to be entirely caused by apoptosis. It is worth noting that Lukinova et al. (30) revealed that iron chelators can alleviate blue light-triggered cell death in ARPE-19 cells, and the research by Argun et al. (11) showed that blue light can induce depletion of intracellular GSH. Moreover, Scimone et al. (31) revealed that blue light can trigger the alteration of ferroptosis-related proteins HMOX1, SCL7A11 and GCLM by omics analysis. Therefore, we speculate that ferroptosis may be the core molecular mechanism of blue light-triggered retinal degeneration and damage. Encouragingly, the results showed that blue light significantly up-regulated intracellular Fe^{2+} levels, leading to ROS burst, accumulation of lipid peroxides (LPOs), cell death, and retinal degeneration (Figs. 1 and 4-5), which was consistent with our speculation.

High-level intracellular Fe^{2+} can generate abundant ROS through

Fenton action, and ROS can further react with polyunsaturated fatty acid-containing phospholipids (PUFA-PL) from the membrane, leading to phospholipid peroxidation and eventually cell death (32). As a core ferroptosis inhibitor, GPX4 can reduce intracellular LPOs to the corresponding alcohols in a GSH-dependent manner, thereby reducing the accumulation of LPOs (14,33). In this study, we found that when retinal cells were treated with blue light, the intracellular GSH levels reduced and the GPX4 expression was suppressed, indicating that the GSH-GPX4 system was disrupted by blue light in retinal cells (Figs. 3 and 6). Moreover, Doll et al. (17) and Bersuker et al. (18) reported a GPX4-independent ferroptosis regulatory pathway, FSP1-CoQ_{10}-NADH. As a type of oxidoreductase, FSP1 can resist excessive lipid peroxidation and ferroptosis by maintaining intracellular redox balance by increasing the consumption of CoQ_{10} and NADH in retinal cells, which has been demonstrated in a recent study by Yang et al. (34). Therefore, we further studied the influence of blue light on the FSP1-CoQ_{10}-NADH system, and the results indicated that blue light significantly inhibited FSP1 expression, increased NADH consumption, and reduced CoQ_{10} activity (Fig. 3). Moreover, in an in vivo model of blue light-triggered retinal degeneration, FSP1 expression was also suppressed, NADH depletion increased and CoQ10 activity was reduced (Fig. 7), which was consistent with the in vivo results. Taken together, these pieces of evidence indicated that blue light disrupts the GSH-GPX4 and FSP1-CoQ_{10}-NADH systems, which further supported our speculation that blue light induces ferroptosis in retinal cells.

To further confirm that ferroptosis did involve in blue light-induced retinal degeneration, deferoxamine (DFO, an FDA-approved iron chelator) was used to pretreat ARPE-19 cells. It turned out that intracellular ROS level and accumulation of LPOs significantly decreased and cell death was alleviated when the Fe^{2+} level was inhibited (Fig. 2). In vivo experiments, considering that DFO may trigger retinal iron deficiency and cause retinal toxicity (35), another ferroptosis inhibitor, Fer-1, was used. As anticipated, Fer-1 significantly reduced the Fe^{2+} level, ROS burst and LPOs accumulation in the retina, and improved retinal degeneration (Figs. 4 and 5). Taken together, these pieces of evidence confirmed that ferroptosis is the core molecular mechanism in blue light-triggered retinal degeneration.

GSH-GPX4 and FSP1-CoQ10-NADH are antioxidant systems known to be mainly associated with ferroptosis and play an essential role in the anti-ferroptosis process (34). In this study, we demonstrate for the first time that blue light has an inhibitory effect on these two antioxidant systems in the retina. Moreover, our results showed that DFO and Fer-1 were able to rescue blue light-induced retinal cell death, which further confirms that Fe^{2+} overload is a key factor contributing to retinal cell death (Fig. 2(G)-2(I)). Notably, as a Fe^{2+} chelator, DFO significantly inhibited the intracellular ROS burst and LPOs accumulation, suggesting that blue light-induced Fe^{2+} overload did cause oxidative stress and oxidative damage in the retina (Fig. 2(C)-2(F)). This study originally revealed the role of ferroptosis in blue light-triggered retinal degeneration and confirmed that ferroptosis is a key molecular mechanism of blue light-induced retinal degeneration. This research assists us in better comprehending the potential mechanisms of retinal photodamage caused by blue light and provides new insights into the prevention of retinal damage caused by blue light pollution or other retinal diseases. However, the present study has some limitations, for example, it has been shown that blue light can induce other types of cell death, including necroptosis (36) and pyroptosis (37), but the relationship between these cell deaths (necroptosis, pyroptosis and ferroptosis) is still unclear. Moreover, it is also unclear whether intermittent blue light exposure has similar biological effects on the retina as continuous blue light exposure.

Ethics approval and consent to participate

Animal experiments were approved by the Ethics Committee of Lanzhou University (EAF 2021001).

Funding

Not applicable.

CRediT authorship contribution statement

Xuan Li: Conceptualization, Formal analysis, Methodology, Investigation, Resources, Writing - original draft. **Sen Zhu:** Resources, Validation, Writing – review & editing, Supervision, Project administration. **Fujian Qi:** Visualization, Investigation.

Declaration of Competing Interest

The authors declare that they have no known competing financial interests or personal relationships that could have appeared to influence the work reported in this paper.

Data availability

Data will be made available on request. The data used to support the findings of this study are available from the corresponding author upon request.

Acknowledgements

Not applicable.

References

[1] R. Fuller, et al., Pollution and health: a progress update, Lancet Planet Health 6 (2022) e535–e547.
[2] D.B. Moyano, Y. Sola, R.A. González-Lezcano, Blue-light levels emitted from portable electronic devices compared to sunlight, Energies 13 (2020) 4276.
[3] F. Behar-Cohen, et al., Light-emitting diodes (LED) for domestic lighting: any risks for the eye? Prog. Retin. Eye Res. 30 (2011) 239–257.
[4] S. Zhu, et al., Hydrogen sulfide protects retina from blue light-induced photodamage and degeneration via inhibiting ROS-mediated ER stress-CHOP apoptosis signal, Redox Rep. 27 (2022) 100–110.
[5] K. Totsuka, et al., Oxidative stress induces ferroptotic cell death in retinal pigment epithelial cells, Exp. Eye Res. 181 (2019) 316–324.
[6] S.G. Jarrett, M.E. Boulton, Consequences of oxidative stress in age-related macular degeneration, Mol. Asp. Med. 33 (2012) 399–417.
[7] J.X. Tao, W.C. Zhou, X.G. Zhu, Mitochondria as potential targets and initiators of the blue light hazard to the retina, Oxidative Med. Cell. Longev. 2019 (2019), 6435364.
[8] W. Li, Y. Jiang, T. Sun, X. Yao, X. Sun, Supplementation of procyanidins B2 attenuates photooxidation-induced apoptosis in ARPE-19 cells, Int. J. Food Sci. Nutr. 67 (2016) 650–659.
[9] J.H. Feng, et al., Cynaroside protects the blue light-induced retinal degeneration through alleviating apoptosis and inducing autophagy in vitro and in vivo, Phytomedicine 88 (2021), 153604.
[10] S. Wang, et al., 17β-estradiol ameliorates light-induced retinal damage in Sprague-Dawley rats by reducing oxidative stress, J. Mol. Neurosci. 55 (2015) 141–151.
[11] M. Argun, et al., Melatonin and amfenac modulate calcium entry, apoptosis, and oxidative stress in ARPE-19 cell culture exposed to blue light irradiation (405 nm), Eye (Lond.) 28 (2014) 752–760.
[12] S.J. Dixon, et al., Ferroptosis: an iron-dependent form of nonapoptotic cell death, Cell 149 (2012) 1060–1072.
[13] C. Han, et al., Ferroptosis and its potential role in human diseases, Front. Pharmacol. 11 (2020) 239.
[14] W.S. Yang, et al., Regulation of ferroptotic cancer cell death by GPX4, Cell 156 (2014) 317–331.
[15] K.R. Marshall, et al., The human apoptosis-inducing protein AMID is an oxidoreductase with a modified flavin cofactor and DNA binding activity, J. Biol. Chem. 280 (2005) 30735–30740.
[16] K. Shimada, et al., Global survey of cell death mechanisms reveals metabolic regulation of ferroptosis, Nat. Chem. Biol. 12 (2016) 497–503.
[17] S. Doll, et al., FSP1 is a glutathione-independent ferroptosis suppressor, Nature 575 (2019) 693–698.
[18] K. Bersuker, et al., The CoQ oxidoreductase FSP1 acts parallel to GPX4 to inhibit ferroptosis, Nature 575 (2019) 688–692.
[19] S. Zhu, et al., Lycium Barbarum polysaccharide protects HaCaT cells from PM2.5-induced apoptosis via inhibiting oxidative stress, ER stress and autophagy, Redox Rep. 27 (2022) 32–44.
[20] X. Jiang, B.R. Stockwell, M. Conrad, Ferroptosis: mechanisms, biology and role in disease, Nat. Rev. Mol. Cell Biol. 22 (2021) 266–282.

[21] J. Moon, et al., Blue light effect on retinal pigment epithelial cells by display devices, Integr. Biol. (Camb) 9 (2017) 436–443.
[22] Q. Wei, et al., 17β-estradiol ameliorates oxidative stress and blue light-emitting diode-induced retinal degeneration by decreasing apoptosis and enhancing autophagy, Drug Des. Devel. Ther. 12 (2018) 2715–2730.
[23] J. Kim, K. Cho, S.Y. Choung, Protective effect of Prunella vulgaris var. L extract against blue light induced damages in ARPE-19 cells and mouse retina, Free Radic. Biol. Med. 152 (2020) 622–631.
[24] K.C. Cheng, et al., The role of oxidative stress and autophagy in blue-light-induced damage to the retinal pigment epithelium in zebrafish in vitro and in vivo, Int. J. Mol. Sci. 22 (2021).
[25] C. Ren, et al., MicroRNA-27a promotes oxidative-induced RPE cell death through targeting FOXO1, Biomed. Res. Int. 2021 (2021) 6666506.
[26] H.M. Cho, Y.D. Jo, S.Y. Choung, Protective effects of Spirulina maxima against blue light-induced retinal damages in A2E-laden ARPE-19 cells and Balb/c mice, Nutrients 14 (2022).
[27] C.Y. Shin, et al., Protective effect of *Ribes nigrum* extract against blue light-induced retinal degeneration in vitro and in vivo, Antioxidants (Basel) 11 (2022).
[28] Z. Zhao, et al., Photooxidative damage in retinal pigment epithelial cells via GRP78 and the protective role of grape skin polyphenols, Food Chem. Toxicol. 74 (2014) 216–224.
[29] A. Alaimo, et al., Toxicity of blue led light and A2E is associated to mitochondrial dynamics impairment in ARPE-19 cells: implications for age-related macular degeneration, Arch. Toxicol. 93 (2019) 1401–1415.
[30] N. Lukinova, et al., Iron chelation protects the retinal pigment epithelial cell line ARPE-19 against cell death triggered by diverse stimuli, Invest. Ophthalmol. Vis. Sci. 50 (2009) 1440–1447.
[31] C. Scimone, et al., N-retinylidene-N-retinylethanolamine adduct induces expression of chronic inflammation cytokines in retinal pigment epithelium cells, Exp. Eye Res. 209 (2021), 108641.
[32] M. Conrad, D.A. Pratt, The chemical basis of ferroptosis, Nat. Chem. Biol. 15 (2019) 1137–1147.
[33] I. Alim, et al., Selenium drives a transcriptional adaptive program to block Ferroptosis and treat stroke, Cell 177 (2019) 1262–1279.e1225.
[34] M. Yang, et al., Involvement of FSP1-CoQ(10)-NADH and GSH-GPx-4 pathways in retinal pigment epithelium ferroptosis, Cell Death Dis. 13 (2022) 468.
[35] R. Haimovici, D.J. D'Amico, E.S. Gragoudas, S. Sokol, The expanded clinical spectrum of deferoxamine retinopathy, Ophthalmology 109 (2002) 164–171.
[36] W. Song, R. Zhu, W. Gao, C. Xing, L. Yang, Blue light induces RPE cell necroptosis, which can be inhibited by minocycline, Front. Med. (Lausanne) 9 (2022), 831463.
[37] C. Brandstetter, J. Patt, F.G. Holz, T.U. Krohne, Inflammasome priming increases retinal pigment epithelial cell susceptibility to lipofuscin phototoxicity by changing the cell death mechanism from apoptosis to pyroptosis, J. Photochem. Photobiol. B 161 (2016) 177–183.